

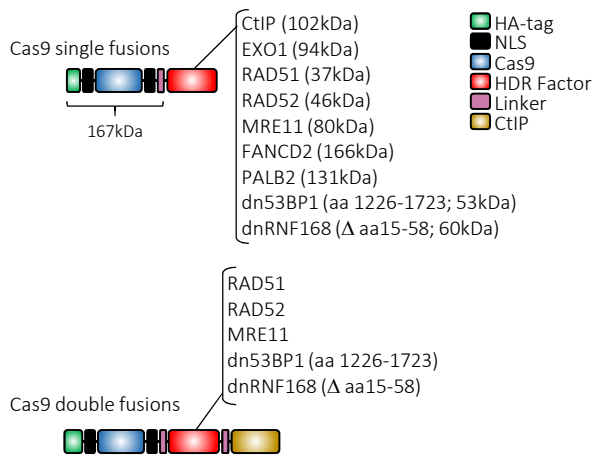
Supplementary Material

A novel Cas9 fusion protein promotes targeted genome editing with reduced mutational burden in primary human cells

Antonio Carusillo, Sibtain Haider, Raul Schäfer, Manuel Rhiel, Daniel Türk, Kay O. Chmielewski, Julia Klermund, Laura Mosti, Geoffroy Andrieux, Richard Schäfer, Tatjana I. Cornu, Toni Cathomen and Claudio Mussolino

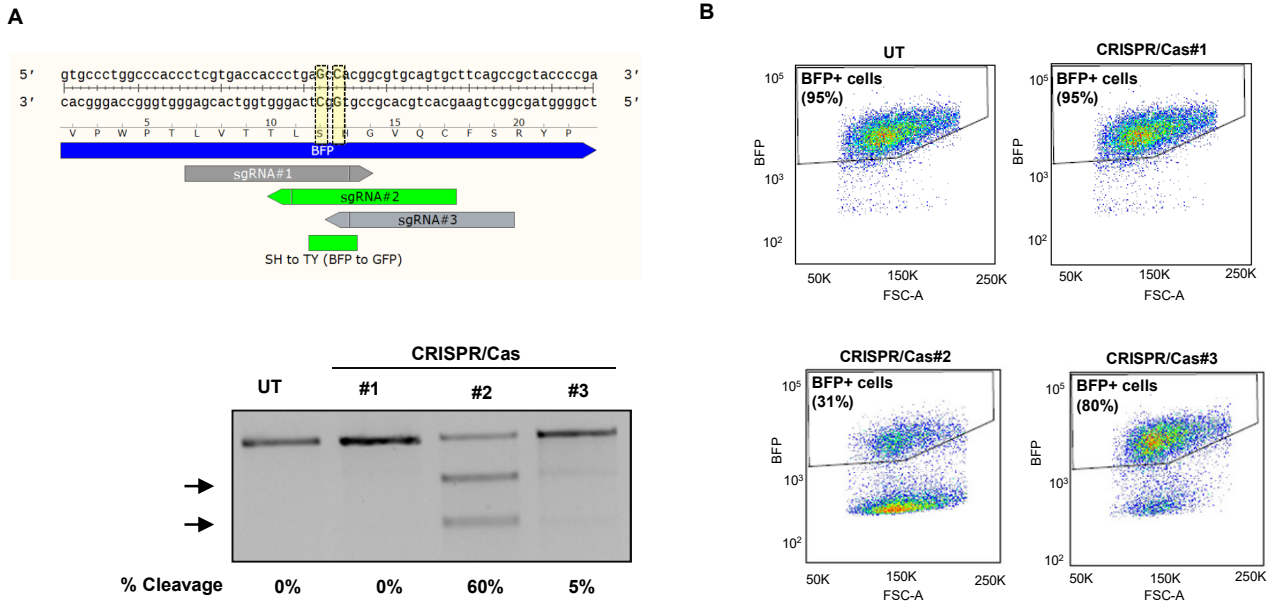
Supplementary Figure 1	Schematic of the Cas9 fusions used
Supplementary Figure 2	Identification of the best performing <i>BFP</i> -specific nuclease
Supplementary Figure 3	Impact of the donor architecture on gene conversion frequency
Supplementary Figure 4	HDR-mediated DSB repair is consistent at different loci and in different cell lines
Supplementary Figure 5	TIDE analysis in K562 upon genome editing using an AAV repair matrix
Supplementary Figure 6	Cas9-CtIP-dnRNF168 does not influence genomic stability
Supplementary Figure 7	HSPCs editing using a dsODN repair template
Supplementary Figure 8	Localization of Cas9-CtIP-dnRNF168 upon DNA damage
Supplementary Table 1	Sequences of ODN repair templates used in this study
Supplementary Table 2	Chromosomal fusions identified via CAST-seq

Carusillo et al., Supplementary Figure 1



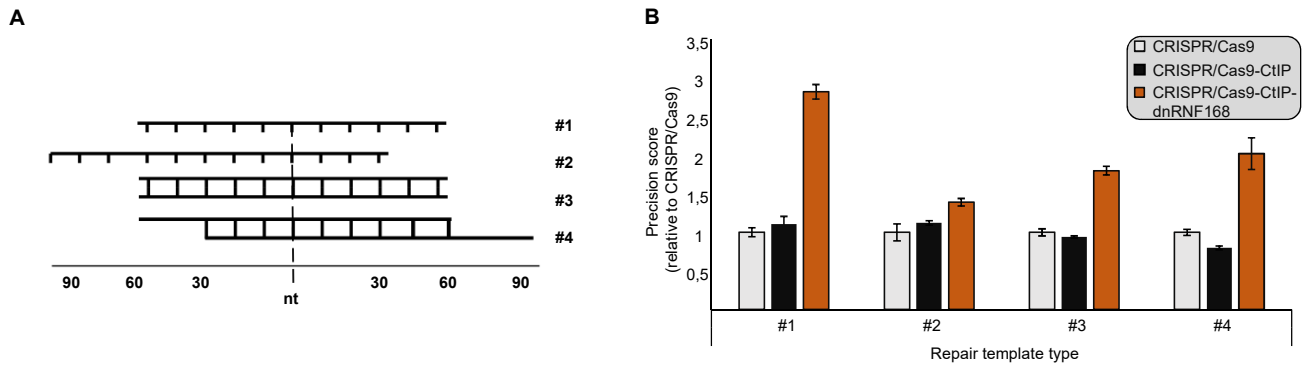
Supplementary Figure 1. Schematic of the Cas9 fusions used. The different components of the Cas9 fusions used in this study are indicated on the right side as colored rectangles. The NHEJ-inhibiting or HDR-promoting proteins used either as single or double fusions to the Cas9 are indicated in brackets. The molecular weight of each effector used is indicated (in kDa). Unless otherwise indicated, each effector is fused to the Cas9 as full-length.

Carusillo et al., Supplementary Figure 2



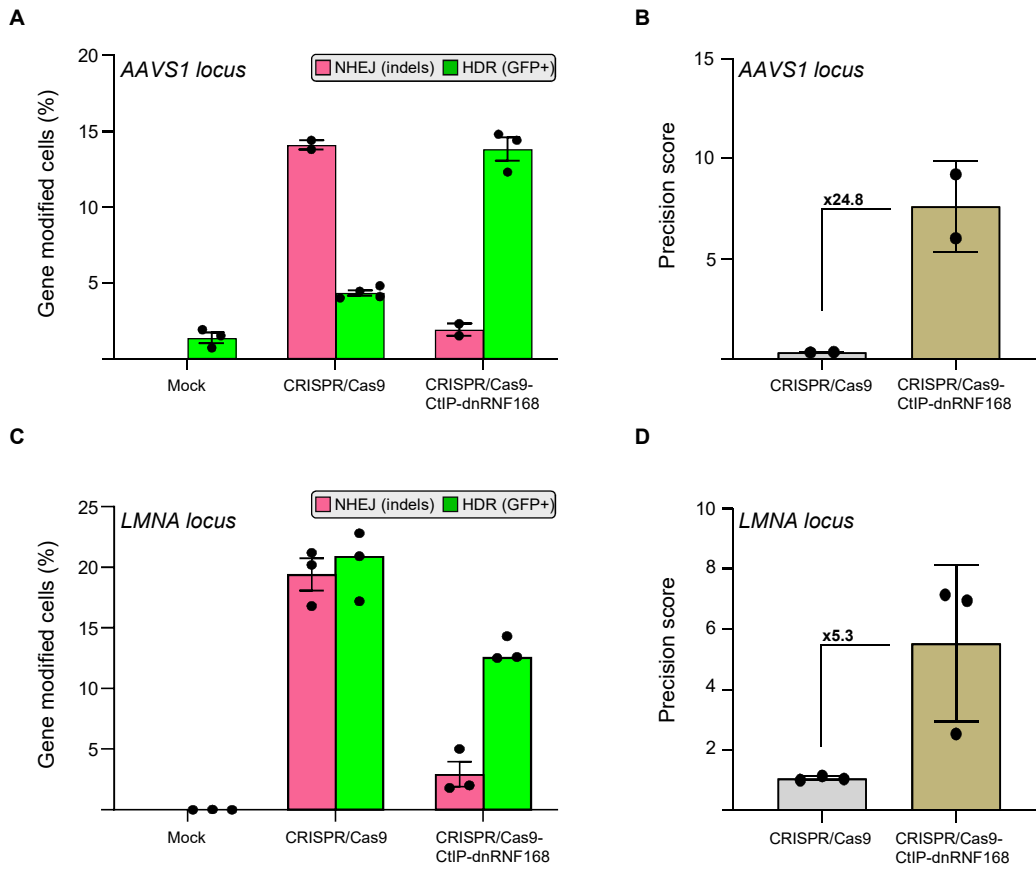
Supplementary Figure 2. Identification of the best performing BFP-specific nuclease

(A) Schematic representation of the *BFP* coding sequence with highlighted the nucleotides responsible for the *BFP*-to-*GFP* conversion and the target sites of the sgRNA included in the *BFP*-specific CRISPR/Cas9 tested (upper panel). The activity of the indicated *BFP*-specific nucleases is monitored via T7 endonuclease 1 assay (lower panel). The arrows indicate the position of the expected cleavage products. The average percentage of modified alleles is indicated below the panel. (B) Exemplary plots showing the targeting efficiency of the different *BFP*-specific nucleases tested measured as reduction in the BFP+ population.



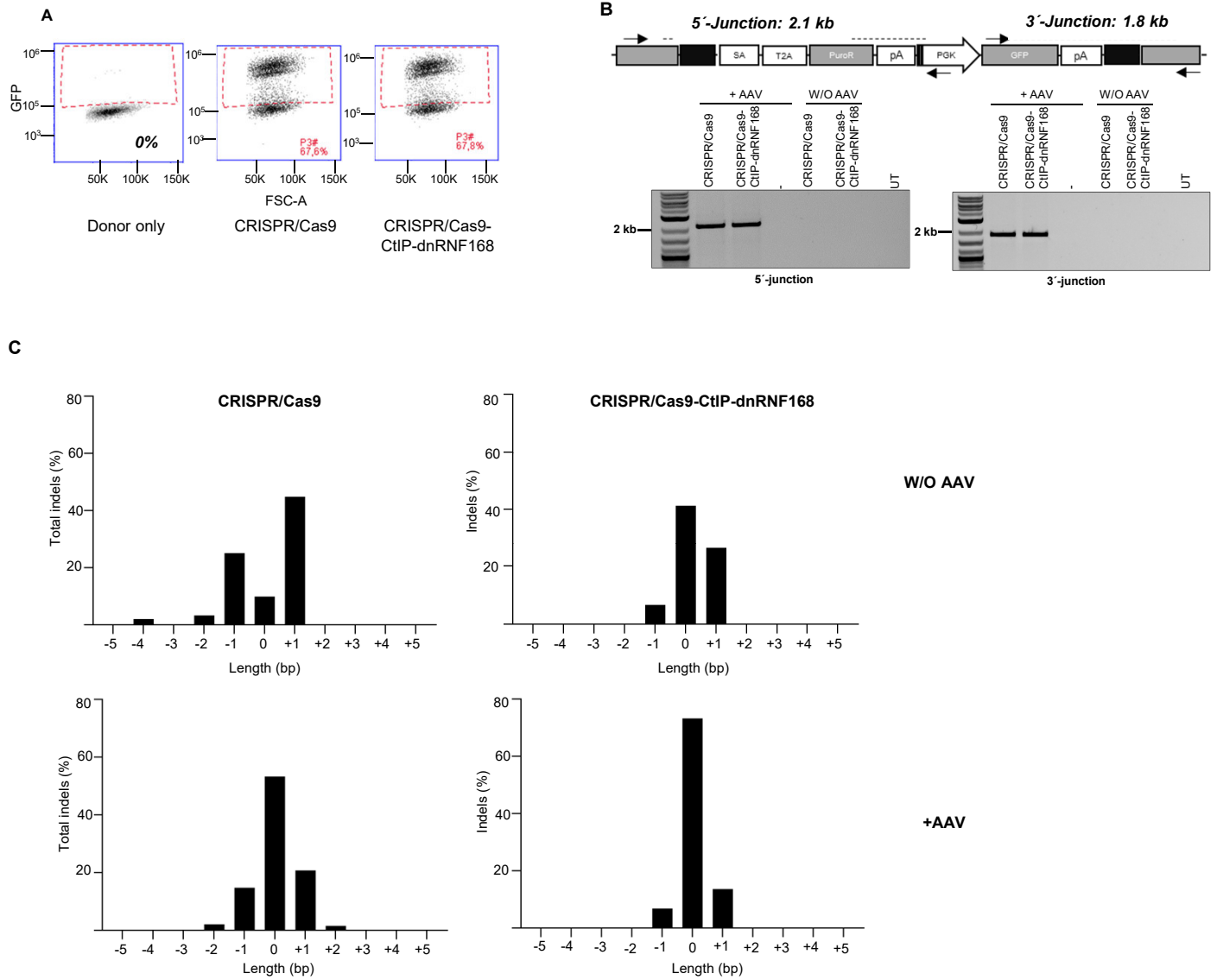
Supplementary Figure 3. Impact of the donor architecture on gene conversion frequency.

(A) Schematic of the different ODN architectures used in the *BFP-to-GFP* assay. The total length of the ODN was kept constant (131nt) and changes include the use of single stranded (#1 and #2) or double stranded (#3 and #4) ODNs with homology arms of the indicated length. nt: nucleotides (B) The bar graph shows the precision score of the indicated nucleases using the ODN indicated below and calculated as fold change relative to the unmodified Cas9.



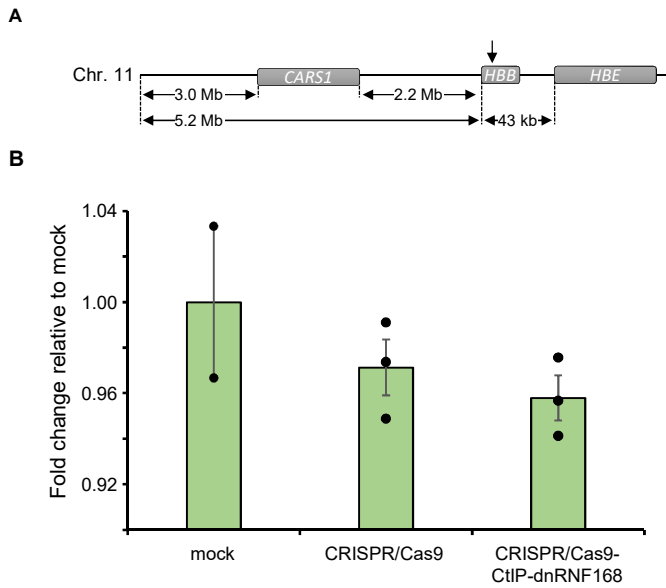
Supplementary Figure 4. HDR-mediated DSB repair is consistent at different loci and in different cell lines.

Targeted integration frequency of a green fluorescent protein (GFP) expression cassette at the *AAVS1* locus in K562 cells (**A**, **B**) or a Clover expression cassette at the *LMNA* locus in HEK293T cells (**C**, **D**). The bar graphs on the left indicate the percentage of NHEJ or HDR events as determined by TIDE or flow cytometry, respectively. The graphs on the right show the precision score, computed as the ratio between the HDR and NHEJ events measured as reported on the left, for the indicated CRISPR system. Each dot represents a biological replicate. Error bars indicate SEM.



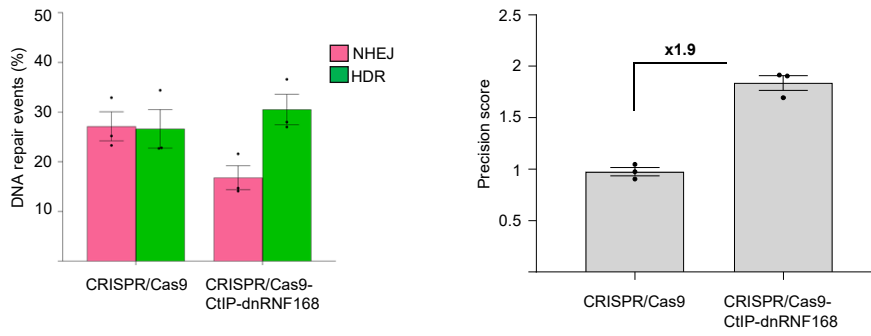
Supplementary Figure 5. TIDE analysis in K562 upon genome editing using an AAV repair matrix.

(A) Representative plots showing the amount of cells expressing a stably integrated GFP expression cassette nine days after electroporation of the indicated nucleases followed by transduction with the AAV repair matrix. (B) Schematics of the in-out PCR strategy used to determine the correct integration of the transgene at the *AAVS1* locus (upper panel) and the resulting PCR products resolved on 2% agarose gel (lower panel). (C) The graphs show the length of the different indel mutation identified by TIDE analysis in K562 cells edited with the indicated nucleases. The TIDE analysis shown is representative of three independent experiments. W/O: without AAV.



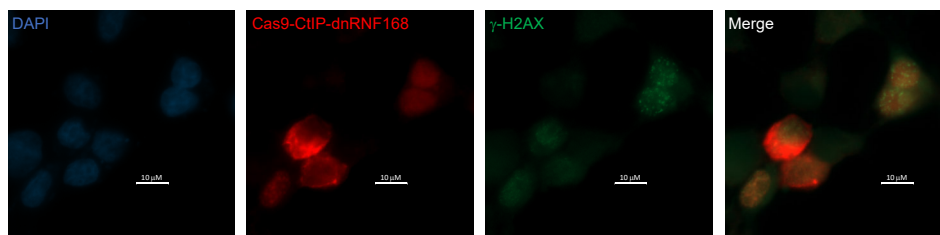
Supplementary Figure 6. Cas9-CtIP-dnRNF168 does not influence genomic stability.

Loss of chromosomal terminal upon CRISPR/Cas activity. (A) Schematic of the terminal p-arm of chromosome 11. The position of the *CARS1* and *HBB* genes relative to the telomere and to the *HBE* gene is shown. The arrow on top indicates the Cas9 cleavage site within the *HBB* gene. (B) Droplet digital PCR is used to estimate the extent of chromosomal terminal loss upon CRISPR/Cas activity. The histogram indicates the fold change relative to the mock control of the ratio between the copy number of *CARS1* and the *HBE* genes located at either sides of the *HBB* target gene. Each dot represents a biological replicate read in triplicate. Error bars indicate SEM.



Supplementary Figure 7. HSPCs editing using a dsODN repair template.

The histograms indicate the frequency of NHEJ- or HDR-mediated DSB resolution assessed via TIDER (left panels) and the corresponding precision score computed as the ratio between the HDR and NHEJ events (right panels) in hematopoietic stem and progenitor cells (HSPCs) edited using a dsODN repair template. Each dot represents a biological replicate. Fold change, as compared to the cells receiving the unmodified Cas9 nuclease, are reported within the graph. Error bars indicate SEM.



Supplementary Figure 8. Localization of Cas9-CtIP-dnRNF168 upon DNA damage.

Representative immunofluorescence staining of HEK293T cells, homogeneously irradiated with 50 Gy, 48 hours after receiving a Cas9-CtIP-dnRNF168 expression plasmid via Lipofection. Staining of phosphorylated γ -H2AX (green) foci is used to visualize irradiation-induced DNA damage, 24 hours after irradiation. Nuclei are stained with DAPI (blue) and the Cas9 is stained with a rabbit anti-HA antibody revealed using an Alexa Fluor 568 goat anti rabbit IgG secondary antibody (red). Scale bars: 10 μ m.

Supplementary Table 1. Sequences of ODN repair templates used in this study

ODN ID	Sequence (5'--> 3') ^{a, b, c}	Purpose
ssODN_#1F	<i>TTCTTCAAGTCC</i> CCCTGAAGTTCATCTGCACCACCGGCAAGCTGCCCGTGCCTGGCCACCCTCGTGACCA <u>C</u> ACTGACCTACGGCGTGCAGTGCTTCAGCCGCTACCCCGACCACATGAAGCAGCACGAC <i>TTCTTCAAGTCC</i>	BFP -to-GFP assay
ssODN_#2F	GCGAGGGCGATGCCACCTACGGCAAGCTGACCCTGAAGTTCATCTGCACCACCGGCAA GCTGCCCGTGCCTGGCCACCCTCGTGACCA <u>C</u> ACTGACCTACGGCGTGCAGTGCTTCA GCCGCTACCCCGAC	BFP -to-GFP assay
ssODN_#3R	GGACTTGAAGAAGTCGTGCTGCTTCATGTGGTCGGGGTAGCGGCTGAAGCACTGCACG CCGT AGG TCAGTGTGGTCACGAGGGTGGGCCAGGGCACGGGCAGCTTGCCGGTGGTG CAGATGAACTTCAGGG	BFP -to-GFP assay
ssODN_#4R	GCGCTCCTGGACGTAGCCTTCGGGCATGGCGGACTTGAAGAAGTCGTGCTGCTTCATGT GGTCGGGGTAGCGGCTGAAGCACTGCACGCCGT AGG TCAGTGTGGTCACGAGGGTGG GCCAGGGCACGGGCA	BFP -to-GFP assay
CCR5_site#1F	<i>TTCTGGGCTCACTATGCTGCCGCCAGTGGGACTTTGGAAATACAATGTGTCAACTCTT</i> G <u>C</u> TAG <u>C</u> GCTCTATTTTATAGGCTTCTTCTCTGGAATCTTCTTCATCATCCTCCTGACAATC GATAG	CCR5 editing
CCR5_site#1R	CTATCGATTGTCAGGAGGATGATGAAGAAGATTCCAGAGAAGAAGCCTATAAAATAGA GC <u>G</u> CT AG CAAGAGTTGACACATTGTATTTCAAAGTCCCCTGCGGCGGCAGCATAGTG AGCCAGAA	CCR5 editing
CCR5_site#2F	TGTCAAGTCCAATCTATGACATCAATTATTATACATCGGAGCCCTGCCAAAAATCAATG TGAAGCAAATCGCAGCCCGC TAG CTGCCTCCGCTCTACTACTGGTGTTTCATCTTTGGTT TTGTGGGCAACATGCTGGTCATCCTCATCCTGATAAACTGCAA	CCR5 editing

^a Homology arms are indicated in italics. The nucleotide changes, as compared to initial sequences, are in bold. The nucleotide changes necessary for PAM disruption are in bold underlined.

^b The dsODNs #3 and #4 in Supplementary Figure 2 derive from annealing ssODN_#1F and ssODN_#3R or ssODN_#1F and ssODN_#4R, respectively

^c The dsODN in Supplementary Figure 4 derive from annealing of CCR5_site#1F and CCR5_site#1R

Supplementary Table 2. Chromosomal fusions identified via CAST-seq[#]

CRISPR/Cas9

chromosome	Type [§]	start	end	read*	hits*
chr3 (on target)	ON	46354559	46388912	3424216	8841
chr22	OMT	29072571	29075210	143442	592
chr13	OMT	24883679	24889410	139765	521
chr19	OMT	35351642	35353222	129119	513
chr16	OMT	3054662	3055266	36925	78
chr1	OMT	31944121	31944708	6174	24
chr6	OMT	34176235	34176890	13986	19
chr22	OMT	42925805	42927384	8626	18
chr5	OMT	172700318	172700854	6423	16
chr15	OMT	64815357	64815881	3173	15
chr10	OMT	11712391	11712940	5527	13
chr9	OMT	34869332	34869838	4368	11
chr11	OMT	70509416	70509930	4843	10
chr19	OMT	35358021	35358530	4940	9
chr19	OMT/HMT	45516296	45516820	4714	9
chr19	OMT	47492202	47492753	2915	9
chr9	OMT	133583476	133584263	4002	8
chr15	OMT	84934931	84935515	6192	7
chr3	OMT	46331188	46332498	2069	7
chrX	OMT	153901851	153902356	8858	5
chr19	OMT	14064757	14065263	4088	5
chr15	OMT	50765350	50765850	2215	2
chr8	HMT	30370457	30372275	745	5
Total:				3.967.325	

CRISPR/Cas9-CtIP-dnRNF168

chromosome	Type [§]	start	end	read*	hits*
chr3	ON	46354471	46379896	1650055	6460
chr22	OMT	29071594	29076155	150913	1071
chr13	OMT	24883679	24888101	67963	491
chr19	OMT	35351646	35353622	47191	403
chr16	OMT	3054662	3055223	7584	28
chr1	OMT	31944127	31946801	18783	74
chr22	OMT	42926691	42927642	8061	45
chr18	OMT	26644196	26646368	10610	45
chr3	OMT	46382788	46389769	4120	19
chr12	OMT	105902012	105902860	1154	13
chr12	OMT	57449620	57450178	4399	12
chr12	OMT	109617835	109618431	2097	11
chr11	OMT	119513944	119514456	4226	7
chr7	OMT	101767757	101768263	2677	6
chr11	OMT	396291	396811	2425	6
Total:				1.982.258	

[#]The sites identified with both nucleases are highlighted in grey.

*The numbers reported result from the sum of two replicate reads

[§]ON: on target; OMT: off target mediated translocation; HMT: homology mediated translocation